Macromolecular Research Article

DOI 10.1007/s13233-017-5121-x www.springer.com/13233 pISSN 1598-5032 eISSN 2092-7673

Fabrication and Characterization of Aligned Fibrin Nanofiber Hydrogel Loaded with PLGA Microspheres

Shenglian Yao[1,2]
Yongdong Yang[2]
Xiumei Wang*[,2]
Luning Wang*[,1]

[1] School of Materials Science and Engineering, University of Science and Technology Beijing, Beijing 100083, P. R. China
[2] School of Materials Science and Engineering, Tsinghua University, Beijing 100084, P. R. China

Received February 28, 2017 / Revised April 15, 2017 / Accepted May 30, 2017

Abstract: Developing novel biomaterials that deliver multiple regulatory signals is crucial to tissue regeneration by creating an ideal regenerative microenvironment. The purpose of the study is to develop a bioactive hydrogel delivering biomimetic joint regulatory cues of low elasticity, aligned structure, and neurotropic factors for nerve regeneration. Here a hierarchically aligned fibrin nanofiber hydrogel (AFG) loaded with drug-encapsulated poly(DL-lactic-*co*-glycolic acid) (PLGA) microspheres (PLGA@AFG) was prepared *via* electrospray and electrospinning. Firstly, drug-nanoencapsulated PLGA microspheres were prepared by electrospray method. Then electrospinning process was used to fabricate the aligned nanofiber hydrogel loaded with PLGA microspheres. Scanning electron microscope (SEM) and laser scanning confocal microscope were engaged to characterize the morphology and drug distribution of the composite hydrogel. The drug release behavior was observed by the use of Congo red as the model drug *in vitro*. The results proved the composite hydrogel maintained the aligned structure and soft properties of the AFG, and achieved a more reasonable drug release behavior for reducing the initial burst release comparing to the PLGA microspheres. Human umbilical mesenchymal stem cells (hUMSCs) were cultured on the PLGA@AFG composite hydrogel. The stem cells exhibited remarkable elongation along the long axis of the AFG with a bipolar morphology, indicating the good biocompatibility of the PLGA@AFG and the regulatory effect of the aligned structure on cell attachment.

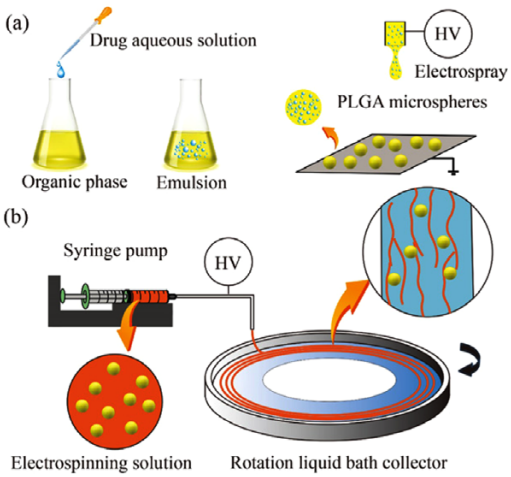

Keywords: aligned nanofiber hydrogel, PLGA microspheres, fibrin hydrogel, drug release, electrospinning.

1. Introduction

In tissue engineering and regenerative medicine, biomaterials are now being designed to display and deliver biochemical, biophysical, and/or biomechanical regulatory signals in a precise and near-physiological fashion to instruct cell fate and induce tissue regeneration. Obviously, a single regulatory signal is still far from satisfactory because of the complicated tissue regeneration processes. Development of novel biomaterials exerting synergistic effects of multiple signals will be beneficial for better regeneration outcomes.

Hydrogels have been widely used as attractive scaffolds in biomedical applications, such as tissue engineering and drug delivery, owing to their unique biocompatibility, flexibility, significant water content, and high permeability for oxygen, nutrients and other metabolites.[1-3] Especially for soft tissues, hydrogels resemble natural extracellular matrix (ECM) more than any other type of polymeric biomaterials. Nerve regeneration is still a worldwide challenge because of the inhibitory microenvironment, which is associated with a series of primary and secondary injury cascades involving damaged neurons, glial scar formation, cystic cavity, neurotrophic factor deficiency, myelin-associated inhibitor accumulation, ischemia, and inflammatory cell infiltration.[4-6] For example, the inhibitory glial scar formed in the injured area plays as a physical barrier and secreted inhibitory factors to inhibit the nerve tissue regeneration.[7,8] Therefore, in nerve tissue regeneration, bioactive hydrogels have been designed with biomimetic softness, aligned topography, bioactive motifs, and/or the encapsulation of neurotropic factors and/or cells.[9]

Matrix elasticity is an important design parameter for simulating the mechanical property of ECM. Hydrogels had notable advantages in the nerve tissue engineering, which have played a positive role in inducing stem cells neurogenic differentiation *in vitro* and nerve tissue invasion *in vivo*.[9] For example, the collagen hydrogel with low elasticity (0.1~1 kPa) could regulate the human mesenchymal stem cells (hMSCs) neurogenic differentiation through the actin protein nonmuscle myosin II.[10] In addition, the aligned structure also works as an important guidance cue in the nerve regeneration. For example, Tuszynski *et al.* constructed a linear channel in the agarose hydrogel that could provide a stable physical passageway to promote axonal regeneration in the injured spinal cord in a highly oriented fashion.[11-14] In comparison

Acknowledgments: This work is in part supported by China Postdoctoral Science Foundation (2016M591075 and 2015M581120), Fundamental Research Funds for the Central Universities (2302016FRF-TP-16-001A1) and Tsinghua University Initiative Scientific Research Program (20161080091, 20131089199).

***Corresponding Authors:** Xiumei Wang (wxm@mail.tsinghua.edu.cn), Luning Wang (luning.wang@ustb.edu.cn)

to the aligned channel structure, the aligned fibers also showed more effective for nerve regeneration, especially the aligned nanofibers, which was demonstrated to induce the stem cells neurogenic differentiation and promote neurite sprouting.[15-19] Therefore, the fabrication of aligned fiber structure (especially in nanoscale) in hydrogel is thought to be useful in nerve tissue engineering by delivering a joint regulatory signals of low elasticity and oriented topography simultaneously. In our previous work, a three-dimensional (3D) aligned fibrin nanofiber hydrogel with oriented structure and low elasticity (~1.5 kPa) was developed *via* electrospinning and a molecular self-assembly process, which showed promoting effects on directing stem cell neurogenic differentiation and rapid neurite outgrowth *in vitro* and *in vivo*.[20]

Besides the biophysical parameters, biochemical signals in the format of bioactive ligands, chemical functionality, and slow-released drugs also should be considered for material design. In nerve regeneration, supplement of neurotropic factors is critical for protecting injured neural cells and stimulating axonal regrowth.[21,22] For example, the chitosan hydrogel loaded the neurotrophin-3 (NT3) provided an excellent microenvironment to facilitate nerve growth, new neurogenesis, and functional recovery of completely transected spinal cord in rats.[23,24] We previously prepared a drug-encapsulated poly(*D,L*-lactic-*co*-glycolic acid) (PLGA) microspheres to deliver angiogenic growth factors (vascular endothelial growth factor (VEGF), angiopoietin-1 and basic fibroblast growth factors (bFGF)) to the lesion site of an injured spinal cord; the results indicated the angiogenic factors could stimulate angiogenesis and neurogenesis, leading to a faster recovery of neurologic function in rats with spinal cord injury.[25] Thus, the delivery of drug in the nerve injured site is an effective approach to improve the nerve regeneration.

Polymeric drug delivery systems (DDS) based on biocompatible and biodegradable polymers are extensively used in recent for the controlled release of single or multiple therapeutic agents.[26] The biodegradable PLGA microspheres have been widely used as a very simple system to obtain ideal controlled release profiles.[27] In our previous work, drug-nanoencapsulated PLGA microspheres were fabricated by emulsion electrospray, with high drug encapsulation efficiency and convenient drug release control.[28] Therefore, the purpose of the study is to develop a bioactive hydrogel delivering biomimetic joint regulatory cues of low elasticity, aligned structure, and neurotropic factors for nerve regeneration.

In this study, the aligned fibrin hydrogel loaded with PLGA microspheres (PLGA@AFG) was fabricated *via* electrospinning and electrospray. Scanning electron microscope (SEM) and laser scanning confocal microscope were engaged to characterize the morphology and drug distribution of the composite hydrogel. Then, the drug release behavior was observed by the use of Congo red as the model drug *in vitro*. Human umbilical mesenchymal stem cells (hUMSCs) were cultured on the PLGA@AFG composite hydrogel to evaluate the bioactivity.

2. Experimental

2.1. Preparation of PLGA microspheres

As our previous work described,[28] poly(*D,L*-lactide-*co*-glycolide), PLGA (Mw 50,000 Da) ether terminated, with a 75/25 ratio (PLA/PGA) from Jinan Daigang Biomaterial Co., Ltd (Shandong, China), was used as biodegradable polymer, and dissolved in chloroform with 6 wt% to form the organic phase. Congo red ($C_{32}H_{22}N_6Na_2O_6S_2$) purchased from Biotopped (Beijing, China) and BSA-FITC (albumin from bovine serum (BSA), fluorescein conjugated from Sigma) were used as model drug to research the water-soluble molecule released behavior and drug distribution. The aqueous phase solution was prepared by dissolving Congo red or BSA-FITC in deionized water. Then, a mixture of aqueous phase and PLGA solution was sonicated (5 cycles, 10 s, 40 W) to form emulsion solution at various volume fraction. Lastly the solution was immediately electrosprayed (<1 h). With a flow rate of 1 mL/h, a high voltage (HV) of 6 kV was supplied to the needle to electrospray. The PLGA microspheres were collected with an aluminum foil with a distance of 20 cm. The schematic illustration of the fabrication process was showed in Figure 1(a). Rhodamine was chosen as the fluorescent marker to label the PLGA microspheres. All the PLGA microspheres were fabricated with 20 μL aqueous phase volume in per milliliter organic solution.

2.2. Fabrication of PLGA@AFG composite hydrogel

Fibrinogen, thrombin, and poly(ethylene glycol) (PEO, average Mw *ca.* 4,000 kDa) were purchased from Sigma Aldrich. Similar to our previous study, briefly, the PLGA microspheres (1 mg/mL) prepared as 2.1 were collected and dispersed into the 10 mg/mL fibrinogen solution in saline with 0.5 wt% PEO to form the elec-

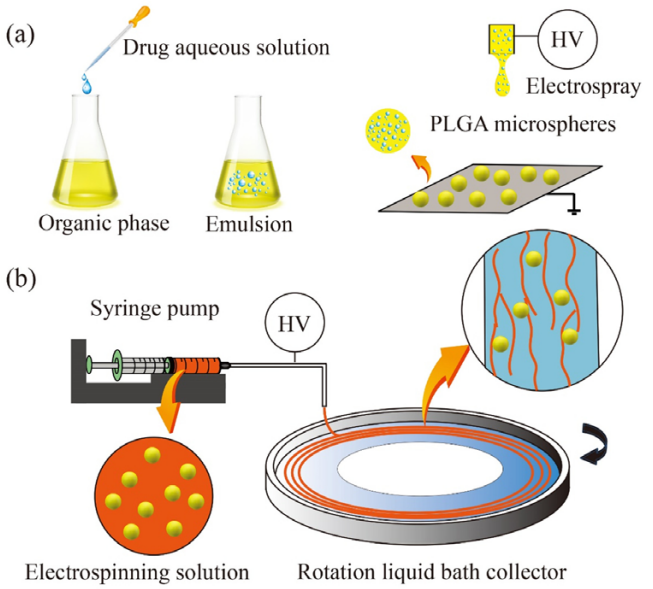

Figure 1. Schematic illustration of PLGA@AFG composite hydrogel fabrication. Two-step were included in this method: the first step was the preparation of PLGA microspheres formed by emulsion electrospray process (a), firstly aqueous phase was added into the organic phase, and then the mixture was sonicated to form emulsion solution, lastly electrosprayed the solution to prepare microspheres; the second step was the electrospinning with rotation liquid bath (b), PLGA microspheres were distributed into the fibrinogen solution, and high voltage was supplied to form a stable electrospinning jet that was landed into the rotation thrombin solution to crosslink and stretch. Finally, the PLGA microspheres were loaded into the aligned fibrin hydrogel to form the PLGA@AFG composite hydrogel.

trospinning solution. As the schematic illustration Figure 1(b) represented, the electrospinning solution was pumped by a syringe with a rate of 1 mL/h, and 3~5 kV positive potential was charged to electrospin. The electrospinning jet was collected by the rotating liquid bath (50 rad/min) with 50 mM of $CaCl_2$ and 5~10 units/mL of thrombin. The jet was crosslinked by the thrombin solution with the PLGA microspheres loaded, and further stretched upon landing in the rotating liquid bath. By this method, the PLGA microspheres were loaded into the aligned fibrin hydrogel to form the PLGA@AFG composite hydrogel as shown in Figure 1(b).

2.3. Morphological observation

2.3.1. PLGA microspheres drug loaded observation

To analyze the distribution of water-soluble molecular drug in the PLGA microspheres, rhodamine was added into the PLGA chloroform organic solution to label the shell of microsphere, and BSA-FITC was used as the model drug. The PLGA microspheres electropun from the syringe were collected by coverslips, and then observed with laser scanning confocal microscope (Zeiss LSM 780, Germany). During the experiment, the Z-stacks model was used to observe the BSA-FITC model drug three-dimensional (3D) distribution, and then the data was analyzed by the software ZEN (Zeiss, Germany).

2.3.2. SEM characterization of PLGA microspheres

The aluminum foil collected PLGA microspheres was cut into 1 cm ×1 cm and drying in air for 24 h. Before the SEM characterization, the PLGA microspheres samples were sputter-coated with a nanoscale Au film. And then, the samples were imaged using a JEOL JSM-7001F field-emission SEM at an accelerating voltage of 10 kV.

2.3.3. SEM characterization of PLGA@AFG composite hydrogel

The PLGA@AFG composite hydrogel and AFG hydrogel samples were fixed with 2.5% glutaraldehyde for 2 h at room temperature, then dehydrated through graded concentrations of ethanol (30%, 50%, 60%, 70%, 80%, 90%, 95%, and 100%), and finally critical point dried with CO_2. Before the SEM characterization, samples were sputter-coated with a nanoscale Au film. And then, the samples were imaged using a JEOL JSM-7001F field-emission SEM at an accelerating voltage of 10 kV.

2.4. Drug release observation

The drug release behavior of PLGA microspheres and the PLGA@AFG composite hydrogel were evaluated as our previous work introduced.[28] Generally, each sample contain 0.2 g PLGA microspheres (both the microspheres and composite hydrogel) was added into a polyethylene pipe (PE) tube vial containing 2 mL of phosphate-buffered saline (PBS) release buffer, and three repeats for each sample group were conducted. All the samples were mounted on a Labquake Rotisserie with 60 rad/min at 37 °C, and at each predetermined time point, 1 mL of the release buffer was collected through centrifuge and replaced by 1 mL fresh buffer. To evaluate the release amount of encapsulated Congo red inside the microspheres/hydrogel, absorption of Congo red under 485 nm (characteristic adsorption wavelength of the Congo red in PBS) was measured using a UV-vis spectrophotometer (Beijing Rayleigh Analytical Instrument Co., China) at room temperature. The Quartz sample cell was sealed up, and the absorption spectra under 485 nm were recorded at same time interval with the reference spectrum of PBS. The drug released rate was calculated by the formula that introduces in the previous work.

2.5. hUMSCs culture and characterization

Primary human umbilical mesenchymal stem cells (hUMSCs) were obtained from Cyagen Bioscience Inc. (Guangzhou, China). hUMSCs were thawed and expanded in growth medium containing α-MEM (Invitrogen), 10% fetal bovine serum (FBS, Gibco), and 1% penicillin/streptomycin (Invitrogen). Cells at passage 6 were used, and cultured on the PLGA@AFG composite hydrogel with the density of 2×10^4 cm^{-2}.

For the observation of adhesion behavior, cells cultured on PLGA@AFG composite hydrogel were fixed in 4% formaldehyde at 4 °C for 2 h. After washed three times with PBS, the samples permeabilized in a solution of 0.1% Triton-X-100 for 5 min. Then, the samples were rinsed with PBS, stained with F-actin marker rhodamine-phalloidin (Dojin, Japan) at room temperature for 40 min, and counterstained with 4',6-diamidino-2-phenylindole (DAPI, Dojin, Japan) for 20 min. After washed three times with PBS, all the samples were observed by a confocal laser scanning microscope (Zeiss LSM 710, Germany). Also the Z-stacks model was chosen and the data analyzed by the software ZEN (Zeiss, Germany).

3. Results and discussion

3.1. Morphology and drug distribution of PLGA microspheres

The drug distribution and surface morphology of PLGA microspheres fabricated by emulsion electrospray were observed by laser scanning confocal microscope (Figure 2(a), (b) and (c)) and SEM (Figure 2(d) and (e)). To visualize the drug distribution in the PLGA microspheres, rhodamine and fluorescence-labeled BSA (BSA-FITC) were used to mark the PLGA shell and water-soluble drug respectively. In the experiment, rhodamine was dissolved into the PLGA chloroform solution, and remained in the PLGA shell homogeneously with the chloroform volatilization during the electrospray process. So the PLGA microspheres could be observed as red spheres by the laser scanning confocal microscope as represented in Figure 2(a). For the BSA-FITC as the water-soluble drug was encapsulated in the PLGA microspheres, the green color in Figure 2(b) represented the drug distribution. As shown in Figure 2(b), the water-soluble drug was nanoparticles and still remained the emulsion morphology in the PLGA chloroform solution. The drug distribution image (Figure 2(b)) was merged with the image of PLGA microspheres (Figure 2(a)) shown in Figure 2(c), which showed that the drug nanoparticles distributed in the whole microsphere without obvious agglomeration.

The morphology of PLGA microspheres was showed in Figure 2(d) and (e). According to the SEM images, PLGA microspheres fabricated by emulsion electrospray were homoge-

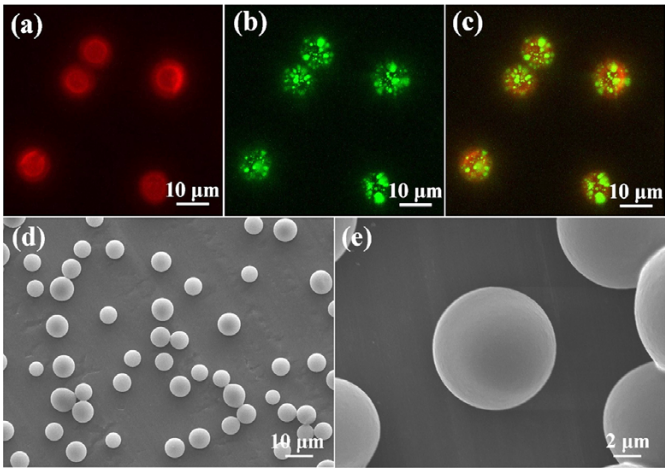

Figure 2. Drug distribution and morphology of PLGA microspheres. The rhodamine labeled the shell of PLGA microspheres was showed in (a), and the BSA-FITC model drug as multiple nanoscale droplets distributed in the PLGA microspheres (b). The PLGA microspheres shell (a) and the loaded drug (b) were merged to show the drug-nanoencapsulated PLGA microspheres (c). (d) and (e) were the SEM images of PLGA microspheres in different magnification.

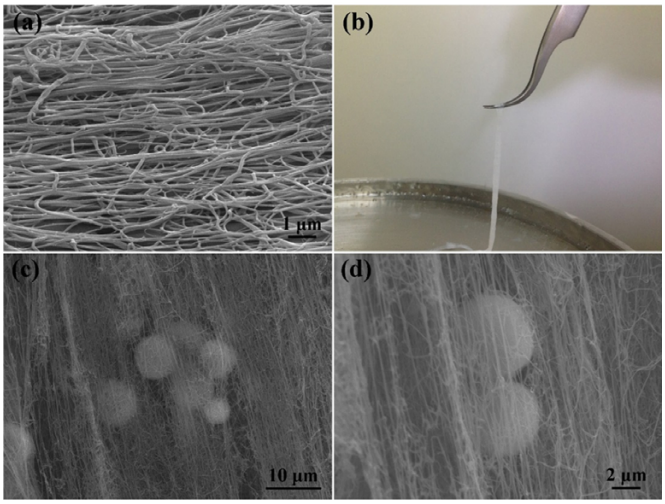

Figure 3. PLGA@AFG composite hydrogel morphology. (a) SEM images of AFG without PLGA microspheres loaded; (b) Gross image of PLGA microspheres-loaded AFG; (c)-(d) SEM images of PLGA microspheres-loaded AFG.

neous with the diameter around 9 μm. The microspheres were spherical shape with smooth surface.

3.2. Fabrication of PLGA@AFG composite hydrogel

As shown in Figure 1, the strategy of PLGA@AFG composite hydrogel fabrication contained two-step, one is the electrospray process to prepare PLGA microspheres, and the other one was the electrostretching process to fabricate the composite hydrogel. In the electrospray process (Figure 1(a)), water-soluble drugs could distribute into the PLGA organic phase by emulsification as nanoscale droplets, and the drug distribution was remained in the subsequent electrospray. Thus, all the water-soluble drugs such as most of proteins could be nanoencapsulated into the PLGA microspheres by this process, and furthermore the drug release behavior could be regulated by controlling the volume ratio of aqueous and organic phase. In the electrostretching process as shown in Figure 1(b), the PLGA microspheres were ultrasonic dispersed into the fibrinogen/PEO solution to form a suspension for further electrostretching. The electrostretching setup was similar to that of electrospinning with the addition of a grounded, motor-driven rotating disc containing a crosslinking solution as the collecting plate. With the addition of rotating disc, the electrospinning jet formed in the electric field could be crosslinked in the liquid bath at a collecting distance about 6 cm. The polymer chain in the electrospinning jet was aligned for the electric field, and would be further stretched in the rotating disc after crosslinking. Thus, aligned fibrin hydrogel could be fabricated, and the diameter also could be regulated by the electrospinning parameter as our previous work introduced. In the electrostretching process, PEO molecules in the solution served as a thickening agent to adjust the viscosity of the electrospinning solution, which could promote a stable electrospinning jet during electrospinning in the electric field. And as a thickening agent, PEO also could improve the stability of PLGA microspheres suspension that was beneficial for the electrospinning and microspheres dispersion. During the second process, the suspended PLGA microspheres in the electrospinning solution didn't affect the electrospinning and crosslinking, for the addition of microspheres would not change the viscosity and electroconductivity of the solution, and also didn't attend to the fibrinogen spontaneous self-assembly crosslinking process. Thus, as the schematic illustration Figure 1 shown, aligned fibrin hydrogel loaded with PLGA microspheres could be fabricated by this two-step method theoretically.

3.3. Characterization of PLGA@AFG composite hydrogel

Through the two-step method, PLGA@AFG composite hydrogel was fabricated as shown in Figure 3(b), (c) and (d). The composite hydrogel was soft and white with high water content (Figure 3(b)). Comparing with the aligned fibrin hydrogel (Figure 2(a)), the alignment structure of fibrin nanofibers was not affected by the addition of PLGA microspheres. The alignment structure of fibrin fibers was mainly decided by the electric field in the electrospinning and the subsequently mechanical stretching in the rotating collector. The addition of microspheres didn't affect the two process obviously. For the PLGA microspheres had fixed into the aligned fibrin hydrogel during the crosslinking reaction, and the subsequent mechanical stretching afforded by the rotating collector couldn't affect the distribution of microspheres to change the fibrin aligned structure.

As shown in Figure 3(c) and (d), the PLGA microspheres could be loaded into the aligned fibrin hydrogel to achieve drug release function. This composite hydrogel had the low elastic moduli and aligned structure of aligned fibrin hydrogel, and was loaded with PLGA microspheres for drug release. That made the PLGA@AFG composite hydrogel as an ideal bioactive materials for the delivery of both physical and chemical signals in neural regeneration.

3.4. Drug release behavior

The drug release behavior of PLGA@AFG composite hydrogel and PLGA microspheres were evaluated to investigate the influence of composite hydrogel on the drug release kinetics. As the results shown in Figure 4, Congo red was used as the model drug and encapsulated in the PLGA microspheres to research the drug release kinetics *in vitro*. For the PLGA microspheres and PLGA@AFG composite hydrogel, there was initial burst release stage within the first 24 h, during which the drug released very quickly. In the initial burst release phase, the cumulative release percentages of Congo red about 32%, which was obviously higher than the PLGA@AFG composite hydrogel (21%). According to the drug distribution within the microspheres, it's obviously that the drug nanoparticles located on/near the shell surfaces of the PLGA microspheres would release out foremost, and this release process last 5 days to reach a stable phase. The PLGA@AFG composite hydrogel reduced the drug release rate obviously in this phase for the fibrin hydrogel around the PLGA microspheres could adsorb the Congo red and work as a barrier for the drug diffusion. And with the fibrin hydrogel degeneration in the release buffer, the adsorbed drug in the fibrin hydrogel released out to increase the release rate form 5 to 20 days. Lastly, only PLGA microspheres remained in both of the two groups, and their drug release behavior were almost the same. The results of Congo red release behavior showed that the PLGA@AFG composite hydrogel could reduce the drug initial burst release rate, and delay the drug nanoparticles located on/near the shell surfaces of the PLGA microspheres diffusing to the release buffer. The fibrin hydrogel was beneficial for the controlling of initial burst release and avoiding the drug over dose in the initial phase.

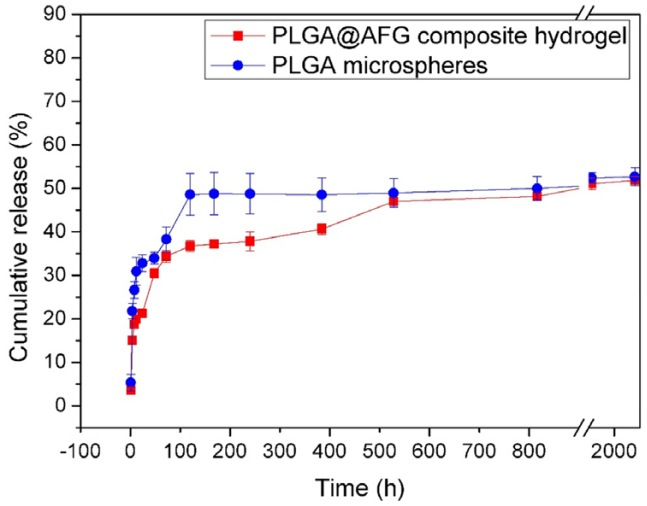

Figure 4. Drug release characteristics of PLGA microspheres and PLGA@AFG composite hydrogel.

3.5. Bioactivity of PLGA@AFG composite hydrogel

The bioactivity of the PLGA@AFG composite hydrogel was characterized by the hUMSCs adhesion behavior. The hUMSCs were cultured on the PLGA@AFG composite hydrogel without aqueous phase drug encapsulation for 1 day in standard culture medium. The cell adhesion morphology was represented by fluorescent staining of cells F-actin and DAPI as shown in Figure 5. The dense cell nucleus stained with DAPI on the PLGA@AFG composite hydrogel demonstrated that the hydrogel could facilitate cell attachment (Figure 5(a)). That because of the fibrin as a natural protein *in vivo* contained two Arginine-Glycine-Aspartate (RGD) integrin-binding sites that was beneficial for the cells adhesion. Furthermore, most of the cell nucleus showed stretching along the hydrogel direction (Figure 5(d)). And the F-actin of hUMSCs on PLGA@AFG composite hydrogel also had highly preferential orientations and were almost parallel to each other with high aspect ratios (Figure 5(b) and (e)). The F-actin and DAPI

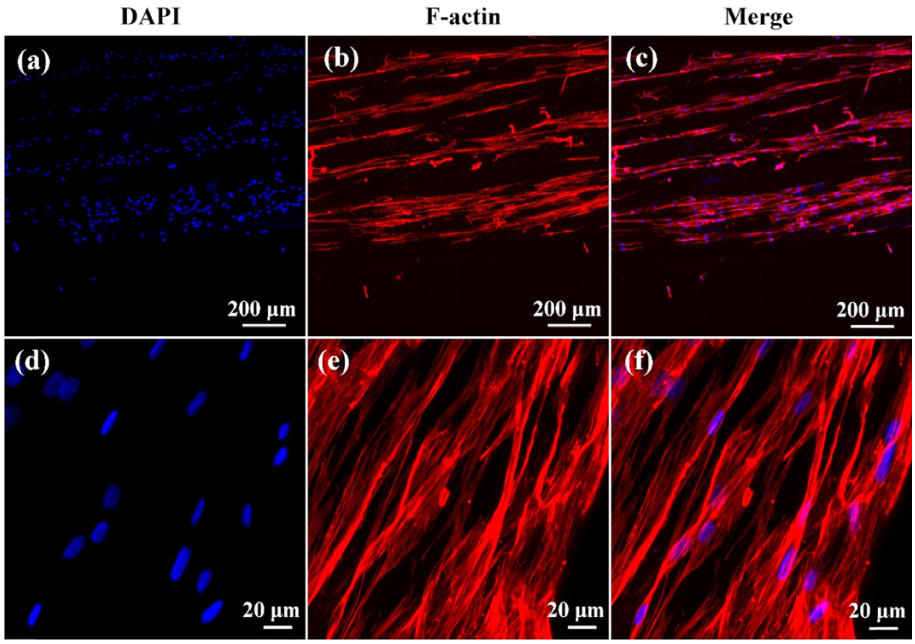

Figure 5. hUMSCs adhesion behavior cultured on the PLGA@AFG composite hydrogel. Typical cell morphologies were represented by fluorescent staining with DAPI for nuclei (blue) ((a) and (d)), and rhodamine-phalloidin for F-actin (red) ((b) and (e)), which were merged in (c) and (f), respectively.

staining were merged in Figure 5(c) and (f), also confirmed the long extension and spindle shaped morphology of hUMSCs on PLGA@AFG composite hydrogel, orienting their axis along and surrounding the aligned fibers in a longitudinal fashion. The cell adhesion results proved the hUMSCs could "feel" the geography of the aligned fibers and adjust their cytoskeletons to align parallel to the fiber direction, and the PLGA microspheres in the hydrogel didn't affect the cell morphology.

In the past few years, researches demonstrated that the stem cell fate decisions can be affected by the cell/material interface, such as nanotopography, stiffness, chemical functionality, soluble factors and degradation by-products.[29] For the stem cells in contact with materials are able to sense their properties, integrate cues *via* signal propagation and ultimately translate parallel signaling information into cell fate decisions.[29] Like the topography and stiffness cues, could be "felt" by the stem cells to control the cell size, shape and polarity through the cytoskeletal proteins.[30] Furthermore, the cytoskeletal rearrangements may lead subsequent changes in intracellular signaling activation. For example, in the Wnt/β-catenin pathway, due to the β-catenin as a structural component of the cytoskeleton as well as mediator of canonical Wnt signaling, it is possible that structural rearrangements in stem cell morphology in response to topography cues could influence the Wnt/β-catenin pathway and regulate the cells behavior.[31] Besides, researches in recent years proved the nucleus could directly "feel" the external cues by the cell actin and microtubules to change the shape, or even gene regulation.[32,33] Our results proved both of the hUMSCs nucleus and actin could be regulated by the PLGA@AFG composite hydrogel, which may induce the hUMSCs neurogenic differentiation as our previous study shown.

To sum up, the PLGA@AFG composite hydrogel combined both of the physical and chemical cues to biomimic the nerve tissue, has the drug release function and cell morphology regulation signals, which have great potential in the neural regeneration.

4. Conclusions

In this work, we report a scalable platform strategy for the generation of PLGA@AFG composite hydrogel with internal alignment and drug release function. Two-step were contained for this strategy, the first step is the electrospray process to prepare PLGA microspheres for nanoencapsulation of water-soluble drugs, and the second one was the electrostretching process to fabricate aligned microfibers hydrogel loaded with PLGA microspheres. The PLGA@AFG composite hydrogel fabricated by this strategy was characterized by SEM and confocal laser scanning microscopy, and the drug release behavior was observed *in vitro*. The results proved the composite hydrogel maintained the aligned structure and soft properties of the AFG, and achieved a more reasonable drug release behavior comparing to the PLGA microspheres. The hUMSCs adhesion behavior demonstrated that the composite hydrogel could induce the cell nucleus and actin to represent spindle shaped morphology along the hydrogel. Thus, the PLGA@AFG composite hydrogel has the drug release function and cell morphology regulation physical signals, which will have great potential in the neural regeneration.

References

(1) B. V. Slaughter, S. S. Khurshid, O. Z. Fisher, A. Khademhosseini, and N. A. Peppas, *Adv. Mater.*, **21**, 3307 (2009).
(2) D. Macaya and M. Spector, *Biomed. Materials.*, **7**, 012001 (2012).
(3) R. Teresa, T. Marta, G. Carmen, G. Antonio, and A. Luigi, *Proc. Inst. Mech. Eng. H J. Eng. Med.*, **229**, 905 (2015).
(4) C. Gumera, B. Rauck, and Y. Wang, *J. Mater. Chem.*, **21**, 7033 (2011).
(5) D. A. Mccreedy and S. E. Sakiyama-Elbert, *Neurosci. Lett.*, **519**, 115 (2012).
(6) C. S. Ahuja and M. Fehlings, *Stem Cells Transl. Med.*, **5**, (2016).
(7) M. V. Sofroniew, *Nat. Rev. Neurosci.*, **16**, 249 (2015).
(8) G. Yiu and Z. He, *Nature. Rev. Neurosci.*, **7**, 617 (2006).
(9) Z. Z. Khaing, R. C. Thomas, S. A. Geissler, and C. E. Schmidt, *Mater. Today*, **17**, 332 (2014).
(10) A. J. Engler, S. Sen, H. L. Sweeney, and D. E. Discher, *Cell*, **126**, 677 (2006).
(11) A. M. Thomas, M. B. Kubilius, S. J. Holland, S. K. Seidlits, R. M. Boehler, A. J. Anderson, B. J. Cummings, and L. D. Shea, *Biomaterials*, **34**, 2213 (2013).
(12) S. Stokols and M. H. Tuszynski, *Biomaterials*, **27**, 443 (2006).
(13) T. Gros, J. S. Sakamoto, A. Blesch, L. A. Havton, and M. H. Tuszynski, *Biomaterials*, **31**, 6719 (2010).
(14) M. Gao, P. Lu, B. Bednark, D. Lynam, J. M. Conner, J. Sakamoto, and M. H. Tuszynski, *Biomaterials*, **34**, 1529 (2013).
(15) L. Tian, M. P. Prabhakaran, and S. Ramakrishna, *Regen. Biomater.*, **2**, 31 (2015).
(16) E. J. Berns, S. Sur, L. Pan, J. E. Goldberger, S. Suresh, S. Zhang, J. A. Kessler, and S. I. Stupp, *Biomaterials*, **35**, 185 (2014).
(17) S. Han, B. Wang, W. Jin, Z. Xiao, X. Li, W. Ding, M. Kapur, B. Chen, B. Yuan, and T. Zhu, *Biomaterials*, **41**, 89 (2015).
(18) V. J. Mukhatyar, M. Salmerónsánchez, S. Rudra, S. Mukhopadaya, T. H. Barker, A. J. García, and R. V. Bellamkonda, *Biomaterials*, **32**, 3958 (2011).
(19) J. Xie, S. M. Willerth, X. Li, M. R. Macewan, A. Rader, S. E. Sakiyamaelbert, and Y. Xia, *Biomaterials*, **30**, 354 (2009).
(20) S. Yao, X. Liu, S. Yu, X. Wang, S. Zhang, Q. Wu, X. Sun, and H. Mao, *Nanoscale*, **8**, 10252 (2016).
(21) H. L. Xu, F. R. Tian, C. T. Lu, J. Xu, Z. L. Fan, J. J. Yang, P. P. Chen, Y. D. Huang, J. Xiao, and Y. Z. Zhao, *Sci. Rep.*, **6**, 38332 (2016).
(22) N. A. Silva, N. Sousa, R. L. Reis, and A. J. Salgado, *Prog. Neurobiol.*, **114**, 25 (2013).
(23) Z. Yang, A. Zhang, H. Duan, S. Zhang, P. Hao, K. Ye, Y. E. Sun, and X. Li, *Proc. Natl. Acad. Sci. U.S.A.*, **112**, 13354 (2015).
(24) H. Duan, W. Ge, A. Zhang, Y. Xi, Z. Chen, D. Luo, Y. Cheng, K. S. Fan, S. Horvath, and M. V. Sofroniew, *Proc. Natl. Acad. Sci. U.S.A.*, **112**, 13360 (2015).
(25) S. Yu, S. Yao, Y. Wen, W. Ying, W. Hao, and Q. Xu, *Sci. Rep.*, **6**, (2016).
(26) F. Ramazani, W. Chen, C. F. van Nostrum, G. Storm, F. Kiessling, T. Lammers, W. E. Hennink, and R. J. Kok, *Int. J. Pharm.*, **499**, 358 (2016).
(27) W. Jiang, R. K. Gupta, M. C. Deshpande, and S. P. Schwendeman, *Adv. Drug Deliv. Rev.*, **57**, 391 (2005).
(28) S. Yao, H. Liu, S. Yu, Y. Li, X. Wang, and L. Wang, *Regen. Biomater.*, **3**, 309 (2016).
(29) W. L. Murphy, T. C. Mcdevitt, and A. J. Engler, *Nat. Mater.*, **13**, 547 (2014).
(30) F. Guilak, D. M. Cohen, B. T. Estes, J. M. Gimble, W. Liedtke, and C. S. Chen, *Cell Stem Cell*, **5**, 17 (2009).
(31) S. H. Lim, X. Y. Liu, H. Song, K. J. Yarema, and H. Q. Mao, *Biomaterials*, **31**, 9031 (2010).
(32) K. N. Dahl, A. J. S. Ribeiro, and J. Lammerding, *Circ. Res.*, **102**, 1307 (2008).
(33) K. Haase, J. K. Macadangdang, C. H. Edrington, C. M. Cuerrier, S. Hadjiantoniou, J. L. Harden, I. S. Skerjanc, and A. E. Pelling, *Sci. Rep.*, **6**, 21300 (2016).

